Amplitude dependent shift of betatron oscillation center

Yoshihiko Shoji,[1] Masaru Takao,[2] and Takeshi Nakamura[2]
[1]Laboratory of Advanced Science and Technology for Industry (LASTI), University of Hyogo, 1-1-2 Kouto, Kamigori-cho, Ako-gun, Hyogo 678-1205, Japan
[2]Japan Synchrotron Radiation Research Institute (JASRI/SPring-8), 1-1-1 Kouto, Sayo, Hyogo 679-5148, Japan
(Received 27 February 2014; published 17 June 2014)

We have analytically calculated and measured the amplitude-dependent shift of the betatron oscillation center at the electron storage ring, NewSUBARU. The shift is due to nonzero average horizontal deflections at the normal sextupole magnets. The shifted center forms a displaced closed orbit and is measured by a closed orbit distortion measurement system, although no single electron runs on this orbit. The measured shifts by betatron oscillations agreed with the theoretical calculation except the variation of data points, which did not obey the ring symmetry. Additional measurements, whose results included the effect of the circumference shift, experimentally proved the amplitude dependent circumference shift for the first time. We also discuss some applications of the shift, which has never been previously analyzed.

DOI: 10.1103/PhysRevSTAB.17.064001 PACS numbers: 41.60.Ap, 29.20.dk, 29.27.Bd

I. INTRODUCTION

A sextupole magnet is an essential element in a synchrotron. On a basic level, it is introduced to control the chromaticity of betatron oscillations. In addition at an advanced level, the sextupole field is considered as a nonlinear element, which limits the dynamic aperture. In particular, the configuration of sextupole magnets is very important in designing recent low-emittance electron storage rings that require strong sextupole magnets. In this paper, on the other hand, we discuss another basic phenomenon—the amplitude-dependent center shift of betatron oscillation, or ADCS. This shift is due to the nonzero average of the horizontal deflection at normal sextupole magnets.

The aim of this paper is to give a simple analytical formula for ADCS and confirm it through measurements. The existence of ADCS is widely acknowledged, but it has never been discussed previously in detail. Although its importance becomes apparent only under special circumstances, ADCS has potential useful applications. One reported application is using the shift to detect beam instability [1]. Another potential application is beam injection with a large oscillation amplitude beam [2]. We will discuss both of these and other applications in the last section of this work.

II. ANALYTICAL FORMULAS

A. Analytical deflection model

In this paper, we will use the conventional coordinates, x, y, and s, as the horizontal displacement, the vertical displacement, and the azimuthal coordinate, respectively. For the other parameters we indicate the direction, horizontal or vertical, by the subscripts $_x$ or $_y$ respectively. We define the normal sextupole component, g, as

$$d\theta_x = (g/2)(x^2 - y^2)ds, \tag{1a}$$

$$d\theta_y = -gxy \cdot ds. \tag{1b}$$

Here, θ_x and θ_y are the horizontal and vertical deflection angles, respectively. We will also use the normalized sextupole components defined by

$$G_x \equiv g\beta_x{}^{3/2}, \tag{2a}$$

$$G_y \equiv g\beta_x{}^{1/2}\beta_y. \tag{2b}$$

Here β_x and β_y are the horizontal and vertical beta functions, respectively.

First, we focus our calculations on the horizontal betatron motion. The linear betatron oscillation is given by

$$x = \sqrt{2J_x\beta_x}\cos\psi_x. \tag{3}$$

Here, J_x is the invariant of horizontal betatron motion and ψ_x is the betatron phase. Substituting Eq. (3) into Eq. (1) we obtain

$$d\theta_x = (g/2)\beta_x J_x(1 + \cos 2\psi_x)ds. \tag{4}$$

The deflection by a sextupole has two frequency components, the constant deflection θ_{x0} and the deflection with twice the betatron oscillation frequency θ_{x2},

$$d\theta_{x0} = (g/2)\beta_x J_x ds, \tag{5a}$$

$$d\theta_{x2} = (g/2)\beta_x J_x \cos 2\psi_x ds. \tag{5b}$$

The constant deflection at $s = s_S$ produces a shift of the oscillation center given by

$$dx_0(s) = \left[\frac{\sqrt{\beta_x(s)\beta_x(s_S)}}{2\sin\pi\nu_x} C_x(s, s_S)\right] d\theta_{x0}. \tag{6}$$

Here, ν_x is the betatron tune and $C_x(s, s_S)$ is the phase factor defined by

$$C_x(s, s_S) \equiv \cos[|\psi_x(s) - \psi_x(s_S)| - \pi\nu_x]. \tag{7}$$

A displacement produced by distributing sextupoles is

$$x_0(s) = \frac{\sqrt{\beta_x(s)}}{4\sin\pi\nu_x} J_x \int_0^L G_x(s_S) C_x(s, s_S) ds_S. \tag{8}$$

The displacement caused by the vertical oscillation with J_y can be calculated by the same manner. Finally, the displacement is given by

$$x_0(s) = \frac{\sqrt{\beta_x(s)}}{4\sin\pi\nu_x} \int_0^L [J_x G_x(s_S) - J_y G_y(s_S)] C_x(s, s_S) ds_S. \tag{9}$$

The oscillating deflection given by Eq. (5b) does not produce any shift of oscillation center. The vertical deflection given by Eq. (1b) has only the oscillating deflection and there exists no vertical shift of oscillation center.

B. Path-length shift and energy displacement

The betatron oscillation also changes the averaged path length for a revolution [3,4]. Then, after a single deflection, the particle would start synchrotron oscillation. The shift of the averaged path length for a revolution is given by

$$\Delta L = -2\pi(\xi_x J_x + \xi_y J_y). \tag{10}$$

Here, ξ_x and ξ_y are the transverse chromaticities. The center of the energy oscillation is given by

$$\delta = (2\pi/\alpha_P L_0)(\xi_x J_x + \xi_y J_y), \tag{11}$$

where α_p is the momentum compaction factor and L_0 is the circumference. Over a long range, averaged over a synchrotron oscillation period, a shift due to the energy displacement of the oscillation center should be added to Eq. (9). That is,

$$x_0(s) = \frac{\sqrt{\beta_x(s)}}{4\sin\pi\nu_x} \int_0^L [J_x G_x(s_S) - J_y G_y(s_S)] C_x(s, s_S) ds_S + \frac{2\pi}{\alpha_P L_0}(\xi_x J_x + \xi_y J_y)\eta(s), \tag{12}$$

where $\eta(s)$ is the dispersion function.

III. MEASUREMENT AT NEWSUBARU

A. Electron storage ring NewSUBARU

We measured ADCS at the electron storage ring, NewSUBARU [5]. Table I shows the parameters of the ring. It is a racetrack shaped ring and has fourfold symmetry. The ring has 44 sextupole magnets divided into four families. The theoretical calculation was based on the ideal ring model, which had a perfect symmetry.

B. Single deflection

We measured ADCS of the horizontal betatron oscillation. A single electron bunch was stored and deflected by an injection kicker magnet. The pulse width of the kicker was 1 μs, which was longer than the twice of the revolution period ($T_{\mathrm{REV}} = 396$ ns). Then the bunch was kicked twice at the successive turns. The turn-by-turn beam position was recorded at 18 beam position monitors (BPMs) in the ring. The measured period was 40 turns after the deflections (16 μs), which was much shorter than the synchrotron oscillation period (190 μs). This means that we measured ADCS given by Eq. (9). The excited oscillation amplitude was $J_x = 1.6$ μm radian. This was obtained from the measured oscillation amplitudes and the beta function from the model. The results are shown in Fig. 1. The measurements agree with the calculation using the ring model and Eq. (9) except the deviation, which does not obey the ring symmetry. This deviation of the data points came from unidentified measurement error because the fitting error itself was the level of the symbol size.

We measured ADCS of the vertical betatron oscillation using a newly installed vertical kicker. The pulse width was 450 ns, which was a little bit longer than the revolution period. The ring was filled with equally spaced 66 bunches. The kicker gave a different vertical oscillation amplitude for each different bunch. The excited oscillation of a bunch

TABLE I. Parameters of NewSUBARU at 1 GeV.

Circumference (L_0)		118.7 m
Synchrotron frequency		5.3 kHz
Betatron tune (ν_x / ν_y)		6.27/2.17
Momentum compaction factor (α_P)		0.00136
Horizontal natural emittance		50 π nm
Chromaticity (ξ_x / ξ_y)	Natural	$-11.1/-6.6$
	with sextupoles	$+2.9/+4.8$

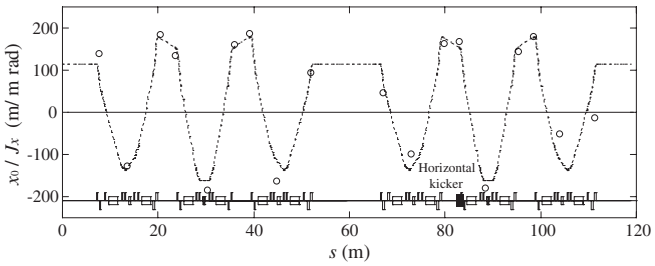

FIG. 1. Horizontal amplitude dependent orbit shift through the ring. The 18 circles are the measured shift at the 18 BPMs and the broken line is the calculated shift using the analytical formula, Eq. (9). The shaded square shows the location of the kicker magnet.

with maximum amplitude was $J_y = 0.07$ μm radian. The multibunch data was used for the analysis to recover the small deflection angle. The oscillation was recorded for 200 turns after the deflection. However we used the initial

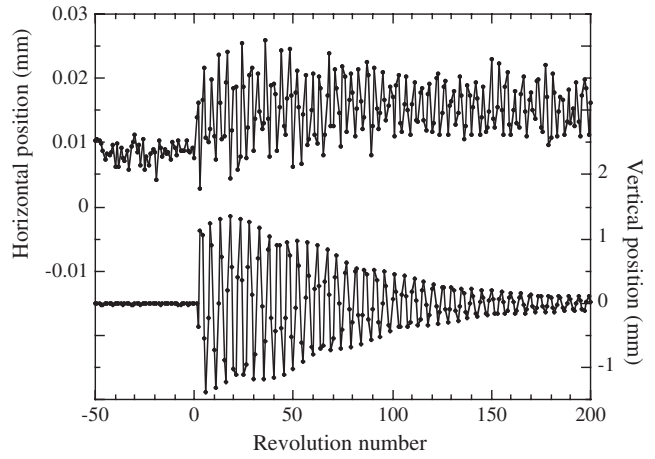

FIG. 2. A typical turn-by-turn beam position in the horizontal (above) and the vertical (below) direction. The deflection took place after the revolution number 0. The vertical oscillation damped because of the chromatic Landau damping. The main component of the horizontal movement after the deflection was horizontal betatron oscillation.

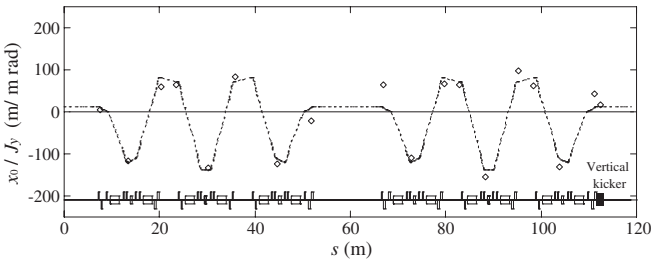

FIG. 3. Vertical amplitude dependent orbit shift. The diamonds are the measured shift at the BPMs and the broken line is the calculated shift using the analytical formula, Eq. (9). One extra data point at the long straight section ($s = 113$ m) was obtained by a newly installed BPM with the new vertical kicker magnet.

40 turns for the analysis to avoid the influence of the orbit drift. Figure 2 shows the example of turn-by-turn beam position signal from one BPM. The measured ADCS are shown in Fig. 3, which agree with the calculation using Eq. (9) except the nonsymmetric deviations.

C. Continuous deflection

We applied continuous deflection to a multibunched beam using the strip-line deflector, which deflected the beam with white noise either in the horizontal or vertical directions. The equilibrium state of the beam is the result of the continuous deflection and radiation damping. In this case, we expect ADCS to be given by Eq. (12).

The increase of the beam spread, produced by the deflection, was estimated from the change of the beam profile. The increase of averaged J_x and J_y were 0.7 and 0.11 μm, respectively. They were calculated using the model beta function at the synchrotron radiation monitor. The orbit shift was measured by means of the slow closed orbit distortion measurement system for 20 times each with the strip-line deflector turned on and off. The difference of beam position in two cases gave ADCS. However, in this case of the continuous deflection, the difference contains a J_x or J_y dependent false signal shift produced by the BPM system. A nonlinear response of BPM and a BPM offset produces a beam size dependent position signal shift. This shift can be calculated using the equation given in the

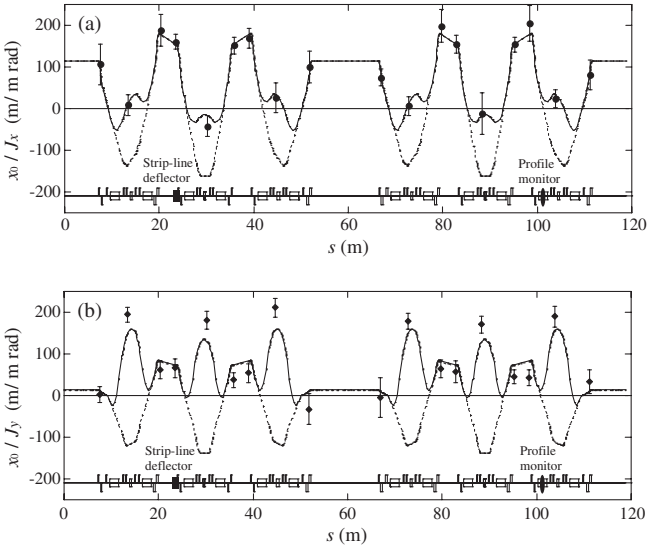

FIG. 4. Amplitude dependent orbit shift by (a) the horizontal betatron oscillation and (b) the vertical betatron oscillation. The circles and the diamonds are the measured shift at the BPMs. The error bars are measurement errors estimated from the variation of 20 measurement results. The broken lines and the solid lines are the calculated shift using the analytical formulas, Eqs. (9) and (12), respectively. The shaded square and the shaded ellipse show the locations of the strip-line deflector and the synchrotron radiation profile monitor, respectively.

Appendix from known parameters, nonlinear response coefficients of BPM, horizontal BPM offset, and beta functions. We subtracted this false shift from the position difference and obtained the ADCS. This false signal was considerable because the BPM had as large as 1.9 mm displacement at the maximum. The results of ADCS measurement, after the correction, are shown in Fig. 4. The differences from the results using the kicker magnets are the first experimental proof of the amplitude dependent "circumference" shift given by Eq. (10).

IV. SUMMARY AND DISCUSSION

We measured ADCS in two different situations, i.e., single deflection and continuous deflection. The results agreed with the theoretical calculations if we ignored the variation, which did not obey the ring symmetry. In the following, we explain examples of application and consequence of ADCS.

At the SPring-8 storage ring, this shift is used to detect any transverse beam instability, which produces an effective beam size blowup. The interlock system, based on the fast rf BPMs, detects ADCS and aborts the stored beam. It protects the front-end components of the photon beam lines from displaced synchrotron radiation. Before the installation of the system using ADCS, we had watched broadband frequency components up to a few hundreds MHz in the fast BPM signal. The strength of these components depended also on the bucket filling pattern, which had no relation with the harmful synchrotron radiation. The old system required a complicated adjustment of the threshold level because the bucket filling was frequently changed at the SPring-8. On the other hand, the ADCS signal is simply proportional to the averaged beam oscillation amplitude and less noisy. The operation became simple and stable with the new system.

ADCS can be considerable at the beam injection, because the oscillation amplitude of the injected beam can be as large as the ring acceptance. Depending on whether the injected beam comes from the outside or the inside according to the sign of the ADCS, the oscillation amplitude can be reduced.

The energy shift given by Eq. (11) can be considerable at beam injection into a quasi-isochronous ring, which has very small α_P. It naturally requires off-energy injection [6]. When the injection point has finite dispersion, the energy displacement can reduce the betatron oscillation amplitude of the injected beam.

Another possible application of the shift is the beam emittance measurement. An intentional ac sextupole field would make $\langle J_x \rangle$ and $\langle J_y \rangle$ dependent orbit oscillation with the ac field frequency. When we have a weak ac sextupole, which produces $x_0/J_x = 1$, it is easy to measure $\langle J_x \rangle$ of nanometer radian. This method does not have any fundamental limitation like diffraction limit of conventional synchrotron radiation profile monitor.

The ADCS is one of the causes of the amplitude dependent tune shift, but it is not the only one. The second harmonic deflection θ_{x2} also contributes to the tune shift. It diverges to infinity at the third-integer tune [7].

ACKNOWLEDGMENTS

We thank the operators of NewSUBARU, Dr. Y. Minagawa, Mr. T. Shinomoto, and Mr. Y. Takemura for their help with the experiments. We also thank Dr. C. Mitsuda and Mr. T. Nakanishi of SPring-8, who helped us to install the new power supply developed by them [8] for the vertical kicker system.

APPENDIX: BETATRON AMPLITUDE DEPENDENT FALSE BPM POSITION SIGNAL

This Appendix explains how the measured beam position could have a false shift. When the beam center is displaced from the BPM center, a nonlinear signal response to the beam displacement makes the false shift in BPM signal. This shift is not real and looks like ADCS.

Generally a raw BPM signal is not linear to the real beam position, x and y. This nonlinearity is corrected after the detection of a signal averaged over particles in a bunch. When we represent this nonlinearity by a function f, the measured result of the position, X, is expressed by

$$X = f^{-1}[\langle f(x,y)\rangle]. \tag{A1}$$

The bracket $\langle\rangle$ means taking average over particles measured at a time. In most cases f is an odd function of x and even function of y because of a mechanical symmetry of BPM structure. Then the function is expanded as

$$f(x,y) = x + ax^3 + bxy^2 + \cdots. \tag{A2}$$

Here a and b are coefficients of the function. From now on we ignore the terms higher than the fourth order. Equation (A1) is rewritten as

$$X + aX^3 + bXY^2 \approx \langle x + ax^3 + bxy^2\rangle. \tag{A3}$$

The parameters X and Y are results of the beam position measurement after the nonlinearity correction.

Here we write the position of a particle by a sum of a displacement of beam center and a displacement from the center as follows:

$$x = x_0 + \delta_x, \tag{A4a}$$

$$y = y_0 + \delta_y. \tag{A4b}$$

Here x_0 and y_0 are the displacements of the beam center and δ_x and δ_y are the displacements from the center. Because of the symmetry δ_x and δ_y satisfy the following equations:

$$\langle \delta_x \rangle = \langle \delta_y \rangle = 0, \tag{A5a}$$

$$\langle {\delta_x}^3 \rangle = \langle \delta_x {\delta_y}^2 \rangle = 0. \tag{A5b}$$

Substituting Eqs. (A4a), (A4b), (A5a), and (A5b) into (A3) gives

$$X + aX^3 + bXY^2 \approx x_0 + a{x_0}^3 + bx_0{y_0}^2 + 3ax_0\langle {\delta_x}^2 \rangle + bx_0\langle {\delta_y}^2 \rangle. \tag{A6}$$

The last two terms on the right-hand side give the false shifts. They are

$$3ax_0\langle {\delta_x}^2 \rangle = 3ax_0\beta_x\langle 2J_x \rangle, \tag{A7a}$$

$$bx_0\langle {\delta_y}^2 \rangle = bx_0\beta_y\langle 2J_y \rangle. \tag{A7b}$$

These false shifts are proportional to J_x or J_y and could be misunderstood as ADCS. However, it is not difficult to cancel the effect because the false dependence can be calculated from known parameters, a, b, β_x, β_y, and x_0. Our equations in this Appendix are a simple version of those for the multi-strip-line beam shape monitors, originally demonstrated by Miller *et al.* [9].

[1] T. Nakamura, M. Takao, K. Soutome, J. Schimizu, K. Kobayashi, T. Seike, and T. Hara, in *Proceedings of the 2nd International Particle Accelerator Conference, San Sebastián, Spain* (EPS-AG, Spain, 2011), pp. 178–180.

[2] Y. Shoji, M. Takao, T. Nakamura, and J. Schimizu, in *Proceedings of the 2nd International Particle Accelerator Conference, San Sebastián, Spain* (Ref. [1]), pp. 2040–2042.

[3] L. Emery, in *Proceedings of the International Conference on High Momentum Accelerators*, edited by J. Rossbach (World Scientific, Singapore, 1993), p. 1172.

[4] Y. Shoji, Phys. Rev. ST Accel. Beams **8**, 094001 (2005).

[5] A. Ando, A. Amano, S. Hashimoto, H. Kinoshita, S. Miyamoto, T. Mochizuki, M. Niibe, Y. Shoji, M. Terasawa, T. Watanabe, and N. Kumagai, J. Synchrotron Radiat. **5**, 342 (1998).

[6] Y. Shoji, Y. Minagawa, and Y. Takemua, in *Proceedings of the 4th International Particle Accelerator Conference, Shanghai, China, 2013*, pp. 1913–1915.

[7] Y.-R. E. Tan, R. Dowd, M. Boland, and D. Appadoo, in *Proceedings of the 23rd Particle Accelerator Conference, Vancouver, Canada, 2009* (IEEE, Piscataway, NJ, 2009), pp. 3711–3713.

[8] C. Mitsuda, K. Fukami, K. Kobayashi, T. Nakanishi, H. Ohkuma, S. Sasaki, and T. Ohshima, in *Proceedings of the 4th International Particle Accelerator Conference, Shanghai, China, 2013*, pp. 666–668.

[9] R. H. Miller, J. E. Clendenin, M. B. James, and J. C. Sheppard, in *Proceedings of the 12th International Conference of High-Energy Accelerators (HEAC'83)* (Fermilab, Illinois, 1983), pp. 602–605.